

Mg based nano-composites fabricated by friction stir processing

C.J. Lee, J.C. Huang*, P.J. Hsieh

Institute of Materials Science and Engineering, Center for Nanoscience and Nanotechnology, National Sun Yat-Sen University, Kaohsiung 804, Taiwan, ROC

Received 1 August 2005; received in revised form 17 November 2005; accepted 21 November 2005

Available online 20 January 2006

Abstract

Friction stir processing (FSP) has been applied to incorporate 5–10 vol.% nano-sized SiO₂ into an AZ61Mg alloy matrix to form bulk composites. The nano-particles were uniformly dispersed after four FSP passes, and the average grain sizes of the composites varied within 0.5–2 μm. The composites nearly doubled the hardness of the base material and exhibited high strain rate superplasticity.

© 2006 Acta Materialia Inc. Published by Elsevier Ltd. All rights reserved.

Keywords: Friction stir processing; AZ61Mg alloy; Nano-particles; Composites

1. Introduction

After the success and gradually wider applications of the friction stir welding (FSW) technique initially developed by The Welding Institute in the UK [1] in joining aerospace aluminum alloys, its recent modification into friction stir processing (FSP) [2,3] has also attracted attention. FSP has been demonstrated to be an effective means of refining the grain size of cast or wrought aluminum based alloys via dynamic recrystallization. A fine grain size typically in the range of 0.5–5 μm in the dynamically recrystallized zone of friction stir processed aluminum and magnesium alloys has been widely reported [2–6]. Extrafine grain sizes in the range of 30–180 nm have also been demonstrated [7]. In addition, Mishra et al. [8] have mixed second phases into the matrix during FSP to fabricate surface composites. There are several methods to fabricate particulate reinforced Al or Mg based composites, including stir casting [9], squeeze casting [10], molten metal infiltration [11], and powder metallurgy [12]. FSP appears to offer another route to incorporate ceramic particles into the metal matrix to form bulk composites.

For most isotropic composites, the micro-sized whiskers or particulates with a reinforcement volume fraction of 15–35% are commonly added into metallic alloys through casting, liquid infiltration or powder metallurgy. In terms of grain size refinement and particle strengthening, one of the critical microstructure parameters is the particle interspacing L , which can be roughly estimated from $L = (\langle d \rangle / 2) (2\pi / 3V_f)^{1/2}$ [13] where $\langle d \rangle$ is the average particle diameter and V_f is the particle volume fraction. With reinforcing particles of $V_f = 20\%$ and $\langle d \rangle = 20 \mu\text{m}$ in typical aluminum based composites, L will be around 32 μm. The resulting grain size after casting would generally fall into this range. Further hot extrusion may refine the grain size down to 5–10 μm. According to the above equation, as the reinforcement size $\langle d \rangle$ decreases to the 10–50 nm range, the composites only need a small volume percentage to result in the interspacing being in the 100–1000 nm range. Upon being subjected to further thermomechanical treatments, the modified alloys might be processed to produce extrafine grain sizes of less than 100 nm [14]. This also suggests that the addition of 3% nano-powders might be able to stabilize the grain size to less than 500 nm at elevated temperatures and enhance superplasticity in the modified alloy [14].

Dispersion of the nano-reinforcements in a uniform manner is a critical and difficult task. A limited number of methods of dispersing the nano-powders have been

* Corresponding author. Tel.: +886 7 5252000x4063; fax: +886 7 5254099.

E-mail address: jacobb@mail.nsysu.edu.tw (J.C. Huang).

disclosed, as most of them are still protected by patents. The current paper presents a simple means of employing FSP to fabricate Mg based nano-composites.

2. Experimental methods

The AZ61A billets used in this study have a chemical composition in mass percent of Mg–6.02%Al–1.01%Zn–0.30%Mn. This alloy is a solution hardened alloy with minimal precipitation. The billet possessed nearly equiaxed grains around 75 μm (based on the linear line intercept method from three cross-sectional planes). The billet was cut as rectangular samples 60 mm in width, 130 mm in length and 10 mm in thickness. Amorphous SiO_2 nanoparticles have an average diameter $\langle d \rangle \sim 20$ nm and purity $\sim 99.9\%$ (Fig. 1). The amorphous SiO_2 particles are nearly equiaxed in shape, with a density of 2.65 Mg/m^3 .

The simplified FSP machine used in this experiment was a modified form of a horizontal-type milling machine, with a 5 HP spindle. The fixed pin tool was 6 mm in diameter and 6 mm in length. The shoulder diameter was 18 mm, and a 2° tilt angle of the fixed pin tool was applied. The pitch distance was 1 mm. The advancing speed of the rotating pin was kept constant in this study to be 45 mm/min, with a fixed pin rotation of 800 rpm. The plates were fixed by a fixture and ambient air cooling was applied. In order to maintain the entire fixture at the initial temperature (room temperature) after each pass, the back plate of the fixture was designed to contain three cooling channels with cooling water passing through them. Using the methods described in a previous paper [6], the strain rate and the maximum temperature experienced during FSP are around 10^1 s^{-1} and 400°C , respectively. To insert the nano- SiO_2 particles, one or two grooves each ~ 6 mm in depth and 1.25 mm in width were cut, in which the nano- SiO_2 particles were filled to the desired amount before FSP. The groove(s) were aligned with the central line of the rotating pin (Fig. 2b). In order to prevent the SiO_2 from being displaced out of the groove(s), surface “repair” was accomplished with a modified FSP tool that only had a shoulder and no pin. The volume fractions of the SiO_2

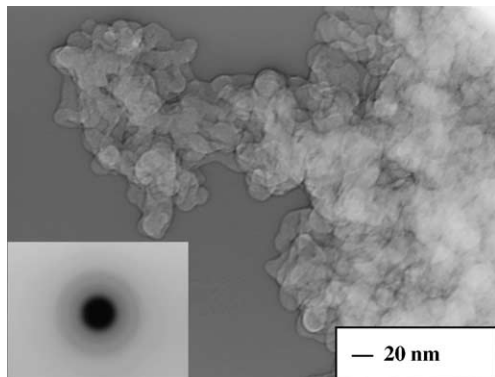


Fig. 1. TEM micrograph and diffraction pattern of the amorphous 20 nm SiO_2 particles.

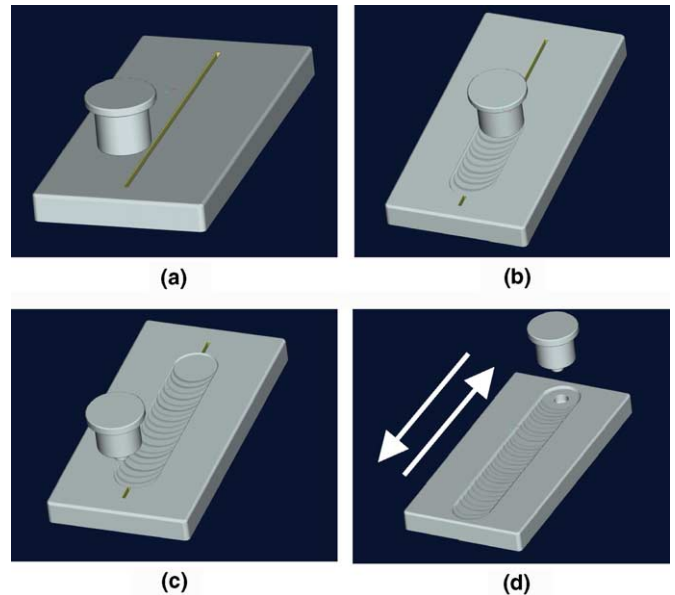


Fig. 2. The FSP procedure: (a) cutting groove(s) and inserting SiO_2 particles; (b) using a flat tool to undertake the surface repair; (c) applying a tool with a fixed pin to undertake the FSP; and (d) conducting multiple FSP passes.

nano-particles inserted into the AZ61Mg alloy were calculated to be around 5% and 10% for the one and two deep grooves (1D and 2D), respectively.

Vickers hardness tests were conducted using a 200 gf load for 10 s. The grain structures and the particle distribution of etched and unetched specimens were examined by optical microscopy (OM), and scanning or transmission electron microscopy (SEM or TEM) with energy dispersive spectrometry (EDS). The size of clustering silica was analyzed by Optimas[®] image analysis software in SEM photographs at different magnifications. The texture was examined by X-ray diffraction (XRD) to observe the transverse cross-sectional plane.

3. Results and discussion

3.1. Microstructures

From the transverse cross-sectional view, there is a characteristic onion ring, measuring nearly 6–7 mm in diameter. The nano- SiO_2 particles are predominantly spread in this regime by the vigorous stirring during FSP at the working temperature around 200–400 $^\circ\text{C}$.

After one-pass (1P) FSP, the particle dispersion within the central cross-sectional area of the onion ring regions was macroscopically uniform, as shown in Fig. 3(a) for the one groove specimen (1D1P). However, the observed clustering particle size is frequently 0.1–3 μm (Table 1), much larger than the individual SiO_2 size (~ 20 nm). The situation after two to four passes (2P, 3P, and 4P), with opposite FSP directions for the following pass (i.e. back and forth), appears to have further reduced the clustering SiO_2 size, as shown in Fig. 3 for the 1D4P and 2D4P spec-

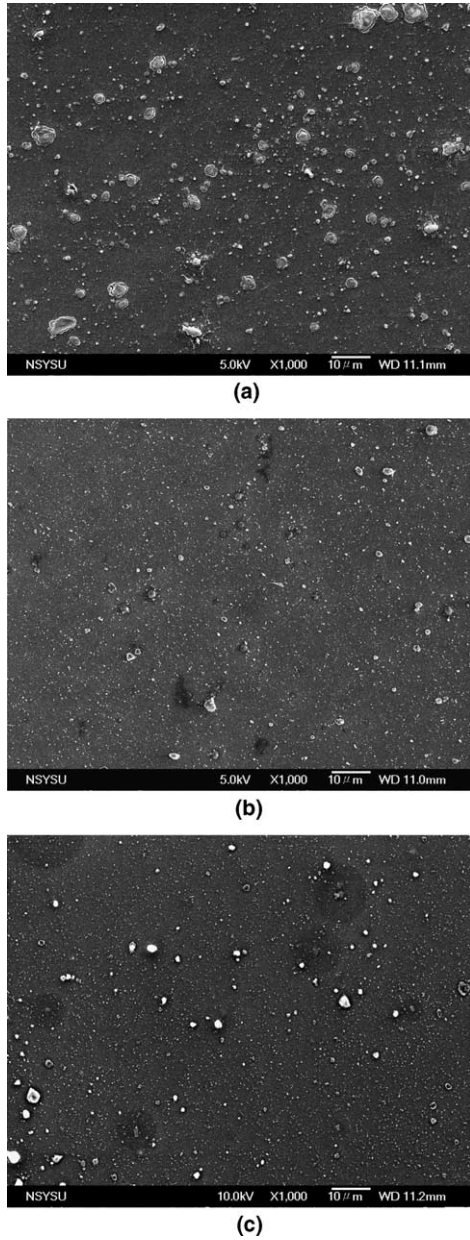


Fig. 3. SEM micrographs showing the particle dispersion: (a) 1D1P ($V_f \sim 5\%$); (b) 1D4P ($V_f \sim 5\%$); and (c) 2D4P ($V_f \sim 10\%$). Some large Al_4Mn phase in distinctly white contrast, measuring 1–3 μm in diameter, can also be seen.

Table 1

Summary of the average SiO_2 cluster size and the average AZ61 matrix grain size in the 1D (with $V_f \sim 5\%$) and 2D (with $V_f \sim 10\%$) FSP specimens

	1D1P	1D2P	1D3P	1D4P
SiO_2 cluster size (nm)	600	210	210	190
Average grain size (μm)	3.1	2.8	2.0	1.8
	2D1P	2D2P	2D3P	2D4P
SiO_2 cluster size (nm)	300	200	170	150
Average grain size (μm)	1.5	1.5	1.0	0.8

The individual SiO_2 size is 20 nm and the initial AZ61 billet grain size is 75 μm .

imens. At higher magnifications, these clustered silica particles are situated on the grain boundaries or trip junctions, and some are embedded inside the grains, as shown in Fig. 4. The size of clustered silica becomes smaller and smaller with increasing FSP passes, as is evident from the statistic data in Fig. 5. Some of the large particles, 1–3 μm in diameter, were identified by SEM–EDS to be Mn bearing dispersoids. The dispersoids are mostly likely Al_4Mn formed in the AZ61 billet during semi-continuous casting.

The typical grain sizes of the composites, estimated using both SEM and TEM micrographs, with 5% and 10% SiO_2 in volume fraction after four FSP passes are 1.8 and 0.8 μm , respectively (Table 1). The resulting grain size is significantly refined from the initial grain size of 75 μm for the AZ61 billet. If all of the SiO_2 nano-particles are completely and uniformly dispersed, the theoretically estimated grain size should vary within 0.1–0.2 μm . It follows that a certain level of local clustering is inevitable, and not all nano-particles can restrict grain boundary migration (Fig. 4). Note that the typical grain size of the AZ61 alloy (without nano- SiO_2 particles) after the same

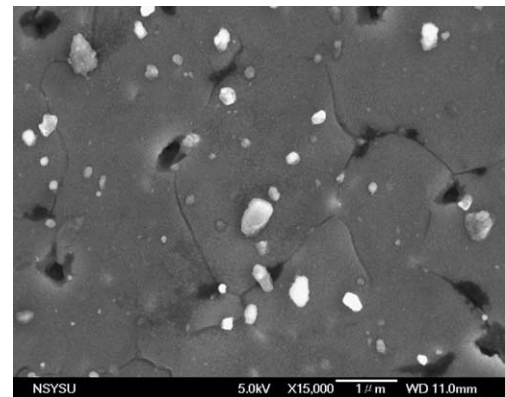


Fig. 4. SEM photograph of the 2D4P specimen showing clustered silica located on grain boundaries or triple junction and some silica embedded in the matrix grains.

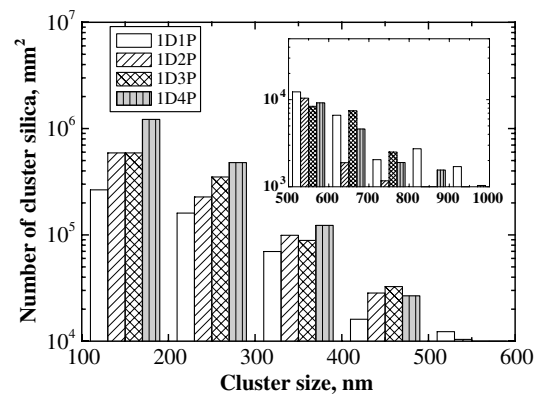


Fig. 5. Statistical results for the clustered silica in the central regime of the 1D specimen after 1–4 FSP passes. Both 1D and 2D specimens showed the same trend.

4P FSP was measured to be around 7–8 μm in our separate studies. The microstructures in the FSP specimens with nano-SiO₂ fillers can be refined to a much smaller scale than the parent alloy.

3.2. TEM phase identification

Fig. 6 presents typical TEM micrographs of the composite specimens. The grain size was estimated by the image analysis software and the data are presented in Table 1. Within the grain interior, tangled dislocations and SiO₂ particles measuring around 10–100 nm can be seen.

The nano-SiO₂ particles maintained their amorphous nature, suggesting that they were not transformed to a crystalline phase during the elevated temperatures experienced during FSP. Experiments to confirm this have been conducted by thermally annealing the amorphous SiO₂ at 430 °C for 10 min (which is higher in temperature and longer in time duration than that experienced during FSP), and still no crystallization was traced by XRD. Occasionally, the TEM diffraction patterns contained multiple rings, which were identified by the d-spacing to originate from MgO fine particles measuring around 5–10 nm (Fig. 7). The MgO phase is formed partly during FSP and partly during TEM foil preparation. After multiple passes, say 3 or 4, some SiO₂ particles would react with

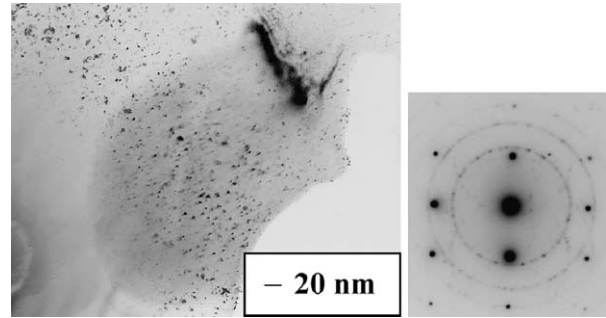


Fig. 7. Fine MgO particles formed in the FSP specimens.

the Mg matrix to form Mg₂Si, as shown in Fig. 8. It is suggested that part of the nano-sized silica particles were originally transformed into MgO and Si, and the Mg and Si reacted to form the Mg₂Si compound; both MgO and Mg₂Si phases measuring 5–200 nm would form during FSP.

3.3. XRD results

The XRD patterns for the transverse cross-sectional plane of the friction stir processed composites are presented in Fig. 9. For complete randomly oriented Mg powders, the (10 $\bar{1}$ 1) peak intensity should be double that of the (10 $\bar{1}$ 0) and (0002) peaks. But in the FSP composites,

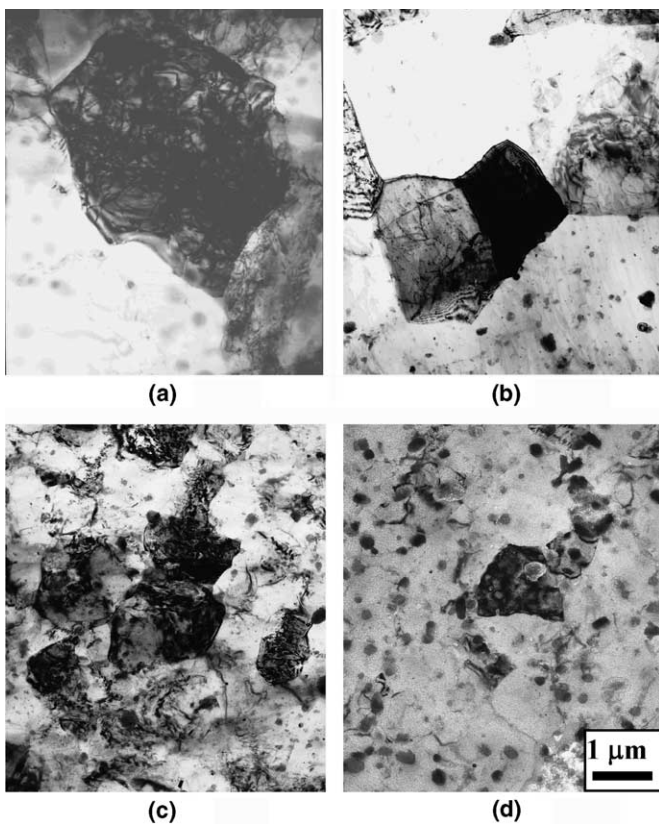


Fig. 6. TEM micrographs showing the matrix grain size and SiO₂ particle distribution in the FSP composites: (a) 1D1P; (b) 1D4P; (c) 2D1P; and (d) 2D4P.

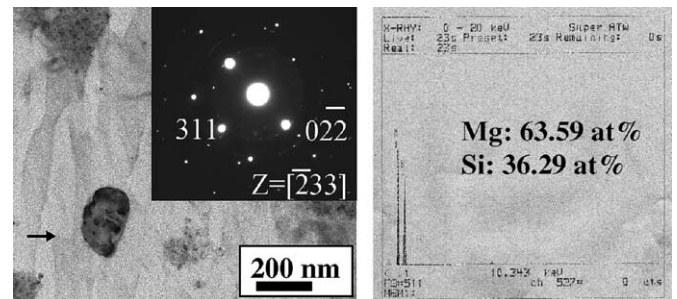


Fig. 8. TEM/EDS results showing the presence of Mg₂Si in the FSP composite specimens.

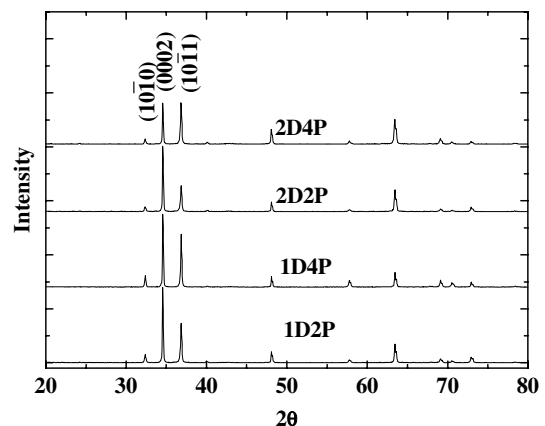


Fig. 9. X-ray diffraction patterns for the 1D and 2D composites after various FSP passes.

the (0002) peak becomes stronger than the (10 $\bar{1}$ 1) peak. This implies that the (0002) basal planes tend to lie on the transverse plane of the friction stir processed specimen (or perpendicular to the pin travel direction). There appears to be a shear stress surrounding the rotating pin during FSP to induce the easiest slip planes of Mg crystal, i.e. the (0002) planes, to align with the shear stress.

XRD results also reveal the presence of Mg₂Si and MgO phases in the composite specimens, as shown in Fig. 10. The peaks related to Mg₂Si are not clear in the 1D specimens, but become more evident in the 2D4P specimens, consistent with the TEM observation. It implies that the SiO₂ particles would gradually react with the Mg matrix with an increasing number of friction stir passes.

3.4. Hardness measurement

The typical microhardness readings, H_v , in the central cross-sectional zones of the friction stir processed specimens are depicted in Fig. 11. The gray regions in the figure represent the groove locations where the silica powders were added into AZ61 before FSP. Almost a double increment of the hardness of the parent AZ61 alloy was

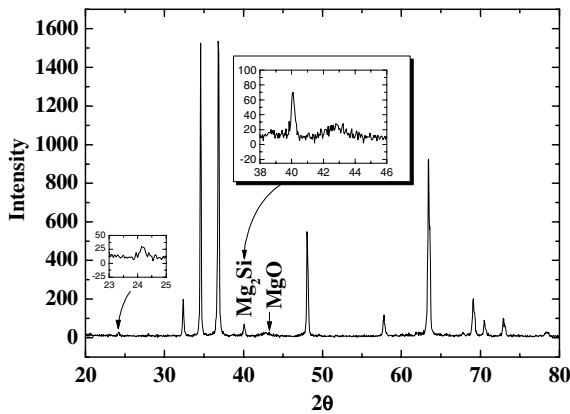


Fig. 10. X-ray diffraction showing the Mg₂Si and MgO phases in the FSP composites.

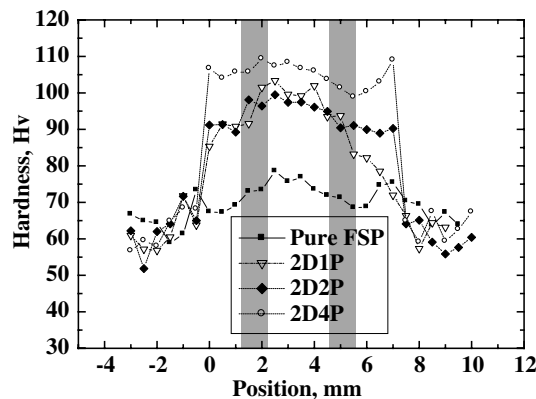


Fig. 11. Typical variation of the microhardness H_v distributions in the AZ61 base alloy (no SiO₂) and composites.

Table 2

Comparison of the mechanical properties of the AZ61 alloy and composites

Material	H_v	YS (MPa)	UTS (MPa)	Elongation (%)
AZ61 billet	60	140	190	13
AZ61 after 4P FSP	72	147	242	11
1D2P ($V_f \sim 5\%$)	91	185	219	10
1D4P ($V_f \sim 5\%$)	97	214	233	8
2D2P ($V_f \sim 10\%$)	94	200	246	4
2D4P ($V_f \sim 10\%$)	105	225	251	4

YS: yield strength; UTS: ultimate tensile strength.

achieved, especially for the 2D specimens with 10 vol.% SiO₂, as compared in Table 2. After FSP, the scattering of H_v within the FSP nugget zone is considered to be minor, implying that the pin stirring efficiently dispersed the nano-silica powders in a reasonably uniform manner, especially after more than one-pass. For the AZ61 alloy with no silica powder, after FSP, the H_v hardness could also increase from ~ 60 up to ~ 72 due to grain refinement from 75 μm down to 7–8 μm via dynamic recrystallization.

3.5. Mechanical properties

Room temperature tensile samples were machined parallel to the welding direction. Table 2 also lists the tensile properties of the FSP alloy and composites, taking the average from two to three specimens. The yield stress of the FSP alloy and composites was improved to 214 MPa in the 1D and to 225 MPa in the 2D specimens, compared with 140 MPa of the as-received AZ61 billet and 147 MPa of the friction stir processed AZ61 alloy without silica reinforcement. The ultimate tensile strength is also appreciably improved in the composite specimens.

The tensile elongation of the 2D4P composites at 350 °C reaches 350% at $1 \times 10^{-2} \text{ s}^{-1}$ and 420% at $1 \times 10^{-1} \text{ s}^{-1}$, clearly exhibiting high strain rate superplasticity (HSRSP). This also implies that the dispersion of the nano-SiO₂ particle is sufficiently uniform, so that extensive elevated temperature deformation can be achieved. However, the tensile elongation at 350 °C and a lower strain rate of $1 \times 10^{-3} \text{ s}^{-1}$ is barely 100%. This interesting HSRSP characteristic will be presented elsewhere.

4. Conclusions

Friction stir processing successfully fabricated bulk AZ61Mg based composites with 5–10 vol.% of nano-SiO₂ particles. The distribution of amorphous SiO₂ nano-particles measuring around 20 nm after four FSP passes resulted in satisfactorily uniform distribution. The grain size of the 2D4P composites could be effectively refined to 0.8 μm , as compared with the 7–8 μm in the FSP AZ61 alloys processed under the same FSP condition. Some SiO₂ reinforcement would react with Mg to form the Mg₂Si and MgO phases during FSP. Nevertheless, both phases are still in the 5–200 nm fine scale. The hardness and

mechanical strength at room temperature of AZ61Mg composites with nano-fillers was strengthened, as compared with the AZ61 cast billet. And high strain rare superplasticity over 400% was achieved in the 2D4P composites.

Acknowledgements

The authors gratefully acknowledge the sponsorship by National Science Council of Taiwan, ROC, under the Project No. NSC 93-2216-E-110-021.

References

- [1] Thomas WM, Nicholas ED, Needham JC, Church MG, Templesmith P, Dawes CJ. The Welding Institute, TWI, International Patent Application No. PCT/GB92/02203 and GB Patent Application No. 9125978.8 1991.
- [2] Mishra RS, Mahoney MW, McFadden SX, Mara NA, Mukherjee AK. Scripta Mater 2000;42:163–8.
- [3] Ma ZY, Mishra RS, Mahoney MW. Acta Mater 2002;50:4419–30.
- [4] Kwon YJ, Shigematsu I, Saito N. Scripta Mater 2003;49:785–9.
- [5] Rhodes CG, Mahoney MW, Bingel WH, Spurling RA, Bampton CC. Scripta Mater 1997;36:69–75.
- [6] Chang CI, Lee CJ, Huang JC. Scripta Mater 2004;51:509–14.
- [7] Su JQ, Nelson TW, Sterling CJ. J Mater Res 2003;18:1757–60.
- [8] Mishra RS, Ma ZY, Charit I. Mater Sci Eng A 2003;341:307–10.
- [9] Saravanan RA, Surappa MK. Mater Sci Eng A 2000;276:108–16.
- [10] Hu L, Wang E. Mater Sci Eng A 2000;278:267–71.
- [11] Han BQ, Dunand DC. Mater Sci Eng A 2000;277:297–304.
- [12] Lee DM, Suh BK, Kim BG, Lee JS, Lee CH. Mater Sci Technol 1997;13:590–5.
- [13] Ardell AJ. Metall Mater Trans A 1985;16:2131–65.
- [14] Wang TD, Huang JC. Mater Trans JIM 2001;42:1781–9.